

Optical breakdown of air triggered by femtosecond laser filaments

Pavel Polynkin^{1, a)} and Jerome V. Moloney¹

College of Optical Sciences, University of Arizona, Tucson, AZ 85721

We report experiments on the generation of dense plasma channels in ambient air using a dual laser pulse excitation scheme. The dilute plasma produced through the filamentation of an ultraintense femtosecond laser pulse is densified via avalanche ionization driven by a co-propagating multi-Joule nanosecond pulse.

PACS numbers: 52.38.-r, 52.25.Jm, 42.65.Jx, 34.80.Gs

Experiments on gas breakdown by powerful optical pulses date back to the early days of lasers¹. The following development resulted in the generation of dense plasma columns up to several tens of meters in length^{2,3}. Pulsed neodymium-glass and CO₂ lasers used in these demonstrations had pulse energies of several hundred Joules. Optical breakdown with high-energy nanosecond (or longer) laser pulses is a threshold-like process with respect to the peak intensity of the pulse. Consequently, the only way of controlling the longitudinal position of the breakdown region that does not rely on adding dust or aerosols locally into the propagation medium is through focusing of the laser beam.

In the last decade, an alternative mechanism of free-charge generation in gases, through femtosecond laser filamentation, has been extensively studied⁴⁻⁶. Differently from breakdown with nanosecond pulses, femtosecond laser filamentation allows for a substantial degree of control over plasma generation in the ambient air. The longitudinal position of the filament can be manipulated by temporally chirping the laser pulse. The placement of the plasma channels within the transverse beam profile can be controlled by beam shaping⁷.

Longitudinally extended plasma channels generated in air through femtosecond laser filamentation could be useful in numerous potential applications. However, the density of free electrons in femtosecond filaments is only about 10^{22} m^{-3} which limits their application space⁸.

It has been suggested that the dilute plasma in femtosecond filaments can be densified through avalanche ionization driven by an additional energetic laser pulse with the duration in the nanosecond range^{9,10}. In this approach, the femtosecond filament acts as a trigger that can be relatively easily controlled, while the nanosecond laser pulse provides sufficient energy for the densification of the plasma channel. In the present Letter, we report the proof-of-principle realization of that proposal.

The combined femtosecond-nanosecond excitation of plasma in gases has been previously used for the generation of dense plasma channels for table-top particle acceleration¹¹ and for Raman amplification of laser pulses¹². The experimental geometries used previously resulted in the generation of, at most, several centimeter-long plasma channels and were not straightforwardly applicable to plasma generation at range.

In the context of filamentation science, experiments on dual-pulse femtosecond-nanosecond excitation have been also reported previously. However, the emphasis has always been on heating, maintenance or revival of the dilute plasma in filaments, not on the direct multiplication of the electrons in the femtosecond filament in an avalanche-like process driven by the nanosecond pulse^{13,14}. In the above works, the femtosecond and nanosecond pulses were separated by a long time interval of up to several milliseconds. In such a situation, the nanosecond pulse liberates the small amount of electrons attached to neutral oxygen molecules in the air filament. The filament can be revived that way, but plasma density in the revived filament remains low.

In the present work, plasma generation occurs in a different regime. The nanosecond heater directly amplifies the free electrons produced through filamentation of the femtosecond igniter pulse. Accordingly, the two pulses in our case are temporally overlapping or nearly overlapping. Our approach results in a substantial boost of the plasma density relative to that in the seed filament.

Let us make some basic estimates. The ionization potentials of oxygen and nitrogen are 12 eV and 16 eV, and their fractional contents in the common air are 21% and 78%, respectively. Thus a complete single-electron ionization of a 1 m - long, 100 μm - diameter air filament will require the expenditure of about 0.5 J of energy from the heater pulse. Commercial Q-switched Nd:YAG lasers are available with pulse energies of up to 50 J, and custom laser systems may deliver yet much higher pulse energies. Thus, from the energy standpoint, the generation of a completely ionized, 100 μm -thick plasma channel or an array of several such channels, with the length of the order of tens of meters, is feasible.

To derive an order-of-magnitude estimate for the required peak power of the heater pulse we assume that, in the laser-driven avalanche, the energy of a free electron in the laser field is increased by one ponderomotive energy on every collision with a neutral or already ionized molecule¹⁵. Through the entire avalanche process, excluding few final electron generations, the densities of both electrons and ions remain low compared to the density of the neutrals. Thus collisions between electrons and ions can be ignored. The rate equation for the energy of a particular electron reads:

$$\frac{d\epsilon(t)}{dt} = \frac{e^2 I(t)}{2c\epsilon_0 m_e \omega_0^2} \cdot f_{em}(t), \quad (1)$$

^{a)}Electronic mail: ppolynkin@optics.arizona.edu

where $I(t)$ is the time-dependent intensity of the heater pulse, e and m_e are electron charge and mass, respectively, c is the speed of light, ϵ_0 is the dielectric constant of vacuum, and ω_0 is the optical frequency. f_{em} is the electron-neutral collision frequency estimated as follows:

$$f_{em}(t) \approx \sigma_{em} N_m \sqrt{2\epsilon(t)/m_e}, \quad (2)$$

where σ_{em} is the collisional cross-section, assumed to be independent of the electron energy. N_m is the density of molecules in the air, which remains approximately constant through the development of the avalanche.

With the exception of the seed electrons provided by the femtosecond filament, the energy evolution for each particular electron, irrespectively to which generation in the avalanche it belongs to, starts from a low value of the order of one ponderomotive energy and ends with the energy approximately equal to the ionization potential E of a neutral molecule. Equation (1) is straightforwardly integrated from 0 to τ , which is the time interval required for an electron to gain energy equal to the ionization potential. (We assume, for simplicity, that all molecules in the air have the same ionization potential.) The result can be written as follows:

$$\tau \approx \frac{2c\epsilon_0 m_e \omega_0^2}{e^2 \sigma_{em} N_m I_0} \cdot \sqrt{2m_e E}, \quad (3)$$

where I_0 is the peak intensity of the heater pulse.

Through the development of the avalanche, the number of free electrons $N_e(t)$ doubles on every avalanche generation, with the doubling period given by the formula (3) above. Thus $N_e(t) = N_0 \cdot 2^{t/\tau}$, where N_0 is the density of the seed electrons. The complete ionization of all air molecules after the passage of the heater pulse means $N_e(T) \approx N_m$, where T is the duration of the heater pulse. Combining this with (3), we find the breakdown threshold intensity of the heater in the form:

$$I_{th} \approx \frac{2c\epsilon_0 m_e \omega_0^2 \sqrt{2m_e E}}{e^2 \sigma_{em} N_m T} \cdot \frac{\ln(N_m/N_0)}{\ln 2}. \quad (4)$$

The ratio of logarithms in (4) equals the approximate number of electron generations required for the complete ionization of air. For a spontaneous (unseeded) optical breakdown of common air, it is estimated¹⁶ that this number is about 40, which corresponds to the seed electron density of the order of 10^{13} m^{-3} . Typical electron density in a femtosecond laser filament in the air is about 10^{22} m^{-3} . If the avalanche is seeded by a filament, the number of electron generations required for the complete ionization is about 11. Thus even though the dependence of the breakdown threshold intensity on the seed electron density is weak (logarithmic), seeding by the filament reduces the threshold intensity by a factor of about 4, a substantial improvement compared to the unseeded case.

For the experimental demonstration of our approach we use the setup shown schematically in Figure 1. The breakdown of ambient air is driven by 10 ns-long heater pulses at 1064 nm wavelength generated by a Q-switched

Nd:YAG laser. The maximum pulse energy of this laser is 3.3 J. The heater pulses are combined with femtosecond igniter pulses at 800 nm wavelength. The igniter pulses are temporally chirped to about 500 fs duration in order to avoid filamentation and associated damage inside the dichroic beam combiner. The heater beam is focused by an axicon lens with the apex angle of 175°. The femtosecond igniter is weakly focused by an ordinary lens with the focal length of 0.5 m. Prior to the lens, the igniter beam is apertured in order to clear a hole made on the axis of the axicon lens used to focus the heater. The maximum energy of the igniter pulse in the filamentation zone is 15 mJ. Prior to focusing, the diameters of the incident heater beam and the apertured igniter beam are 20 mm and 5 mm, respectively. The pointing of the igniter beam is adjusted in order to overlap the seed filament with the ~ 30 cm-long linear focal zone of the axicon. The waist of the igniter pulse is approximately in the middle of the linear focus zone for the heater. Both igniter and heater lasers operate at 10 Hz pulse repetition frequency. The pulse trains from the two lasers are synchronized through a common triggering. The time delay between the pulses is varied by means of an electronic delay unit placed in the trigger path for the heater laser.

With the heater beam turned off, the femtosecond igniter creates an ~ 20 cm-long dilute filament, a photograph of which is shown in the left part of Figure 2. To make this faint filament visible, the image was integrated over about 100 laser shots. No plasma generation is observed when the heater beam is applied at its maximum energy but the igniter beam is turned off. With both igniter and heater pulses applied at their maximum energies and with the temporal delay between the pulses optimized, a seeded optical breakdown is observed reliably on every laser shot. The photograph of the breakdown region is shown in the right part of Figure 2. In this case, the 10 cm - long plasma channel is bright and visible on a single-shot image. Like in the earlier experiments on the longitudinally extended gas breakdown with nanosecond pulses^{2,3}, the generated channel is fragmented into multiple plasma bubbles. In our case, the bubbles are separated by about 1 mm and positioned irregularly along the channel. This fragmentation is a result of the local plasma shielding for the heater beam. Using axicon focusing for the heater beam allows for the reconstruction of the main intensity peak on the beam axis after this peak is locally scattered by the generated dense plasma.

Although the femtosecond filament reliably triggers

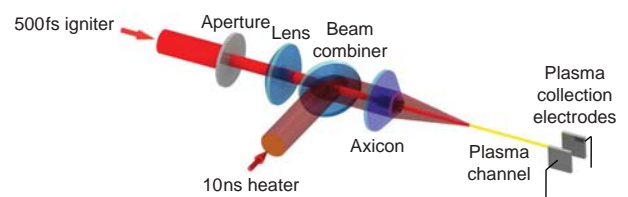


FIG. 1. Experimental setup.

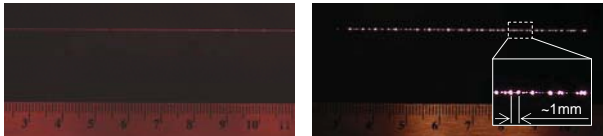


FIG. 2. Left: Multi-shot image of the seed filament. Right: Single-shot image of the dense plasma channel resulting from the joint application of the igniter and heater pulses.

optical breakdown, it does not improve the continuity of the densified plasma channel. The fragmentation of the channel limits the potential utility of this technique. We are investigating potential solutions for this problem by using beam shaping of the igniter laser.

The generated plasma density is quantified, on a relative scale, by using a capacitive plasma probe¹⁷. The probe has $1\text{ cm} \times 1\text{ cm}$ collection electrodes that are separated by 1.5 cm , charged to 100 V , and placed in the middle of the plasma channel.

In the left part of Figure 3, we show the dependence of the plasma density generated through the joint application of the igniter and heater pulses, as a function of the delay between the pulses. Both pulses are at their maximum available energies. The plasma density is shown relative to the density with the heater pulse turned off. The maximum plasma-enhancement factor is about 200.

The dependence of the plasma density enhancement on the energy of the heater pulse is shown in right part of Figure 3. The energy of the igniter pulse is kept at a maximum, and the temporal delay between the pulses is optimized to maximize the signal. A clear threshold with respect to the energy of the heater pulse is evident, as expected. To relate the pulse energy to the peak power density of the heater in the interaction zone, we use the approximate formulas derived for axicon focusing in terms of the input beam diameter and axicon angle¹⁸. In our experimental geometry, the diameter of the extended linear focus for the heater is estimated at $40\text{ }\mu\text{m}$. The enhancement of the heater on-axis intensity due to the focusing by the axicon is about 2,200. Accordingly, the threshold heater energy of about 2.2 J corresponds to

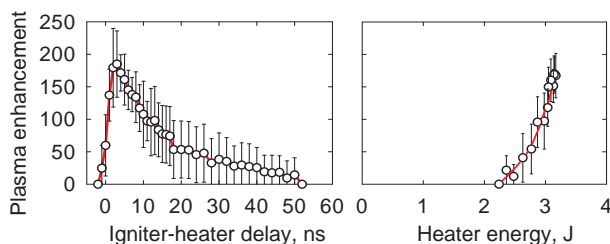


FIG. 3. Left: Plasma-density enhancement relative to the density in the femtosecond igniter filament, vs. time delay between the igniter and heater pulses. The energies of the igniter and heater pulses are 15 mJ and 3.3 J , respectively. Right: Plasma-density enhancement as a function of the heater-pulse energy, at the optimum delay between the pulses.

the peak heater-beam intensity of $1.5 \times 10^{15}\text{ W/m}^2$.

At this point, making a connection between these experiments and the earlier modeling results^{9,10} is not straightforward, because the earlier analyses were based on point models. The fragmentation of the densified plasma channel into bubbles is an important effect both for the practical utility of these channels and for understanding the physics behind dual-pulse plasma excitation. The adequate simulation of our results will require the inclusion of the propagation aspect in the model.

In conclusion, we have conducted experiments on the generation of dense plasma channels in ambient air using the dual-pulse femtosecond-nanosecond excitation scheme. Reliable triggering of the optical breakdown by the femtosecond seed filament was demonstrated. A maximum plasma enhancement factor of about 200 in the dense plasma channel of about 10 cm in length was measured. The densified channels are fragmented into millimeter-scale plasma bubbles which may be a limitation to their utility. Further development of our approach and its scaling to higher energies of the heater pulse may yield a viable technique for the controllable generation of extended plasma channels and channel arrays in the atmosphere that can be useful in many applications.

The authors acknowledge helpful discussions with Ewan Wright. This work was supported by The United States Air Force Office of Scientific Research under programs FA9550-10-1-0237 and FA9550-10-1-0561.

- ¹R. G. Meyerand, A. F. Haught, *Phys. Rev. Lett.* **11**, 401 (1963).
- ²V. A. Parfenov, L. N. Pakhomov, V. Yu. Petrun'kin, V. A. Podlevski, *Sov. Tech. Phys. Lett.* **2**, 286 (1977).
- ³V. V. Apollonov, L. M. Vasilyak, S. Yu. Kazantsev, I. G. Kononov, D. N. Polyakov, A. V. Saifulin, K. N. Firsov, *Quant. Electron.* **32**, 115 (2002).
- ⁴A. Couairon, A. Mysyrowicz, *Phys. Rep.* **441**, 47 (2007).
- ⁵L. Berge, S. Skupin, R. Nuter, J. Kasparian, J.-P. Wolf, *Rep. Prog. Phys.* **70**, 1633 (2007).
- ⁶S. L. Chin, *Femtosecond Laser Filamentation* (Springer, New York, 2010).
- ⁷G. Mechain, A. Couairon, M. Franco, B. Prade, A. Mysyrowicz, *Phys. Rev. Lett.* **93**, 035003 (2004).
- ⁸Y.-H. Chen, S. Varma, T. M. Antonsen, H. M. Milchberg, *Phys. Rev. Lett.* **105**, 215005 (2010).
- ⁹M. N. Shneider, A. N. Zheltikov, R. B. Miles, *Phys. Plasmas* **18**, 063509 (2011).
- ¹⁰P. Sprangle, J. Peñano, B. Hafizi, D. Gordon, M. Scully, *Appl. Phys. Lett.* **98**, 211102 (2011).
- ¹¹P. Volbeyn, E. Esarey, W. Lemans, *Phys. Plasmas* **6**, 2269 (1999).
- ¹²C.-H. Pai, M. W. Lin, L. C. Ha, S. T. Huang, Y. C. Tsou, H. H. Chu, J. Y. Lin, J. Wang, and S.-Y. Chen, *Phys. Rev. Lett.* **101**, 065005 (2008).
- ¹³B. Zhou, S. Akturk, B. Prade, Y.-B. André, A. Houard, Y. Liu, M. Franco, C. D'Amico, E. Salmon, Z.-Q. Hao, N. Lascoux, and A. Mysyrowicz, *Opt. Express* **17**, 11450 (2009).
- ¹⁴Z. Q. Hao, J. Zhang, Y. T. Li, X. Lu, X. H. Yuan, Z. Y. Zheng, Z. H. Wang, W. J. Ling, Z. Y. Wei, *Appl. Phys. B* **80**, 627 (2005).
- ¹⁵Y. B. Zeldovich, Yu. P. Raizer, *Sov. Phys. JETP* **20**, 772 (1965).
- ¹⁶*Principles of Laser Plasmas*, edited by G. Bekefi (Wiley, New York, 1976).
- ¹⁷P. Polynkin, M. Kolesik, A. Roberts, D. Faccio, P. Di Trapani, and J. Moloney, *Opt. Express* **16**, 15733 (2008).
- ¹⁸A. Friberg, *J. Opt. Soc. Am. A* **13**, 743 (1996).